Efficient Transfer of Large-Area Graphene Films onto Rigid Substrates by Hot Pressing

Junmo Kang,[†] Soonhwi Hwang,[†] Jae Hwan Kim,[‡] Min Hyeok Kim,[†] Jaechul Ryu,[†] Sang Jae Seo,[†] Byung Hee Hong,[†,§,*] Moon Ki Kim,[†,‡,*] and Jae-Boong Choi[†,‡,*]

[†]SKKU Advanced Institute of Nanotechnology (SAINT) and Center for Human Interface Nano Technology (HINT), and [‡]School of Mechanical Engineering, Sungkyunkwan University, Suwon, 440-746, Korea, and [§]Department of Chemistry, Seoul National University, Seoul, 151-747, Korea

ABSTRACT

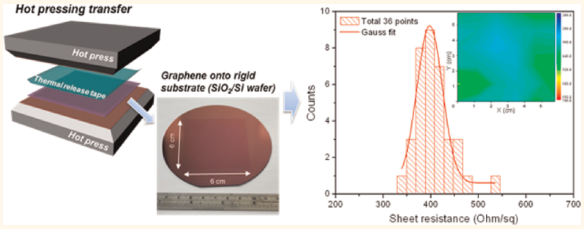

Graphene films grown on metal substrates by chemical vapor deposition (CVD) method have to be safely transferred onto desired substrates for further applications. Recently, a roll-to-roll (R2R) method has been developed for large-area transfer, which is particularly efficient for flexible target substrates. However, in the case of rigid substrates such as glass or wafers, the roll-based method is found to induce considerable mechanical damages on graphene films during the transfer process, resulting in the degradation of electrical property. Here we introduce an improved dry transfer technique based on a hot-pressing method that can minimize damage on graphene by neutralizing mechanical stress. Thus, we enhanced the transfer efficiency of the large-area graphene films on a substrate with arbitrary thickness and rigidity, evidenced by scanning electron microscope (SEM) and atomic force microscope (AFM) images, Raman spectra, and various electrical characterizations. We also performed a theoretical multiscale simulation from continuum to atomic level to compare the mechanical stresses caused by the R2R and the hot-pressing methods, which also supports our conclusion. Consequently, we believe that the proposed hot-pressing method will be immediately useful for display and solar cell applications that currently require rigid and large substrates.

KEYWORDS: graphene · dry transfer · hot pressing · arbitrary substrate · chemical vapor deposition · multiscale analysis

The discovery of graphene has ignited intensive studies on two-dimensional nanoscale materials and their potential applications particularly for transparent electronic components[1−5] due to its extraordinary properties, such as high carrier mobility,[2−4,6] superelastic mechanical behavior,[7,8] and ultraelectrical conductivity with high optical transmittance[9,10] that are important for practical applications.[10−12] Since the first isolation of graphene by mechanical exfoliation,[1] various methods to produce graphene have been devised, including nanomechanical cleavage,[13] chemical oxidation/reduction,[14,15] and direct growth on SiC[16,17] or metal substrates.[9,18,19] Recently, there have been a lot of advances in CVD techniques to grow high-quality large-area graphene films,[9,19] which enabled various electronic applications including touchscreens and organic light-emitting diodes (OLEDs).[9,10,20−22] However, the difficulty in transferring graphene films to desired substrates without critical defects limits the electrical performance of graphene.

Various transfer methods for two-dimensional nanomaterials have been developed.[10,11,23−30] First, micromechanical exfoliation of highly oriented pyrolytic graphite (HOPG) using adhesive tapes was used to prepare micrometer-sized flakes of graphene.[1] The most common transfer method is to use a polymer support such as poly(methyl methacrylate) (PMMA) or polydimethylsiloxane (PDMS) during etching and transfer processes. However, this wet process is not suitable for the preparation of large-scale graphene films because it requires elaborate handling skills and a long time to remove the polymer supports after transfer. The R2R transfer using thermal release tapes (TRT) as temporary supports successfully overcame these drawbacks.[10] In addition, it has enabled the continuous production of graphene films at meter scale on flexible substrates. However, the R2R transfer sometimes causes undesired mechanical defects on graphene films when it is applied to rigid substrates such as SiO_2/Si wafers[24,25] which considerably degrades the electrical properties of resulting graphene films.[23,24]

* Address correspondence to byunghee@snu.ac.kr, mkkim@me.skku.ac.kr, boong33@skku.edu.

Received for review March 19, 2012 and accepted May 27, 2012.

Published online May 28, 2012
10.1021/nn301207d

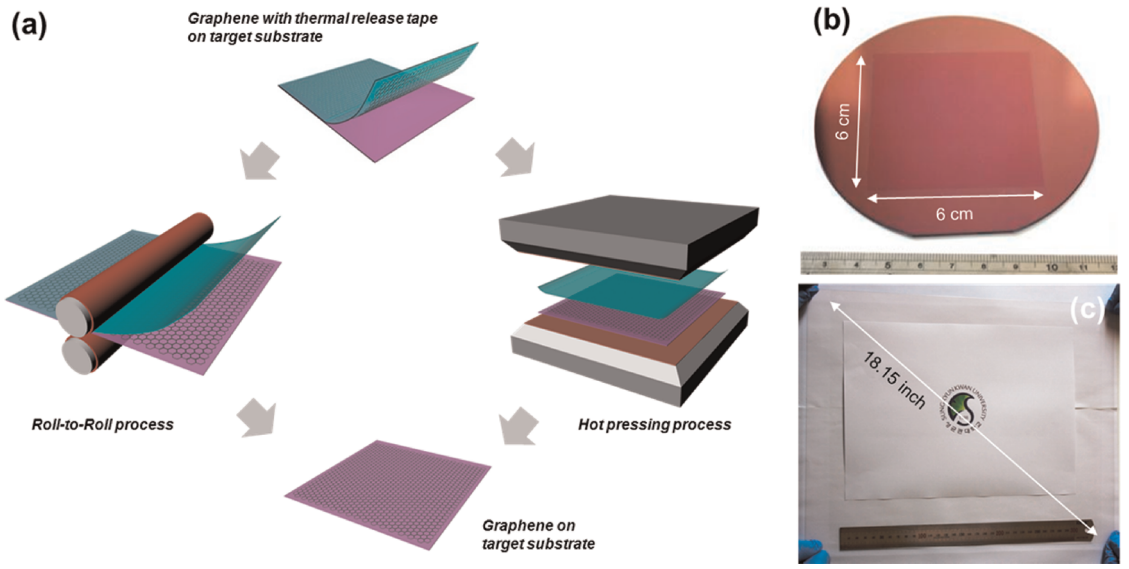

Figure 1. (a) Schematic illustration of graphene transfer by R2R and hot pressing; (b) photograph of a 6 × 6 cm^2 graphene film transferred onto a SiO_2/Si wafer by hot pressing; (c) photograph of an 18-in. graphene film transferred on a glass substrate by hot pressing.

In this work, we report an improved dry transfer method called "hot pressing" that uses two hot metal plates pressing each other with precisely controlled temperature and pressure. The hot pressing method is expected to result in a relatively small number of defects and better electrical property both for flexible polyethylene terephthalate (PET) substrates and rigid SiO_2/Si wafers, which is evidenced by optical microscope images, atomic force microscope (AFM) analysis, scanning electron microscope (SEM) images, Raman spectra, and theoretical analyses of strained graphene from an atomic level to a continuum level.

RESULTS AND DISCUSSION

Figure 1 illustrates the schematic diagram of the dry transfer process of as-grown graphene from a TRT to arbitrary substrates such as PET and SiO_2/Si wafer. The preliminary steps involve graphene growth, attaching graphene on Cu to TRT, and the etching of Cu layers as described in the Experimental Method section. The graphene film on TRT is attached to the target substrate and then transferred by using R2R and the hot pressing processes. In the R2R process, the stacked layer of TRT/graphene/substrate is sequentially exposed to heat under a certain pressure applied between the rollers, while the entire area is heated and pressed simultaneously within 10 s in the hot pressing process. After the transfer process, the TRT can be easily removed as its adhesive force disappears. Thus, we are able to transfer the large-area graphene films on arbitrary substrates up to meter scale. Figures 1 parts b and c show the large-area monolayer graphene films transferred onto a SiO_2/Si wafer and a glass substrate, respectively, by a hot pressing process.

To understand mechanical behaviors of thin-film structures during the dry transfer process, we devised a multiscale simulation framework for the stacked structures of TRTs, graphene films, and substrates based on finite element method (FEM), and the strain distribution of the stacked structures was simulated by a commercial FEM package called ABAQUS. Figure 2 illustrates the typical two-dimensional finite element models and the strain distributions over the TRT/graphene/PET structures during the two different transfer processes, respectively. We assumed that TRT/graphene film/PET is one structure and there exists a friction between the structure and the roller or the plate. The stress−strain curve of nonannealed PET was adopted[31] and utilized in this simulation. While the R2R process with both compressive and shearing loads results in the maximum strain around outer edges, the mechanical loads are uniformly spread over the entire structure in the hot pressing process, which enables more uniform strain distribution as well as less deformation, leading to the better electrical performance of graphene films.

Figure 3 shows graphene films (2 × 2 cm^2) on SiO_2/Si wafer transferred by R2R and hot pressing processes. Figure 3 panels a and b demonstrate the low resolution optical images of monolayer graphene on the SiO_2/Si wafer transferred by R2R and hot pressing, respectively. While the R2R transferred sample contains many line-shaped cracks and large voids with the sizes of 1−5 μm, the hot-pressed sample shows a relatively uniform morphology with less defective structures (Figure 3c,d). In the R2R transferred graphene film, the cracks seem to propagate perpendicular to the rolling direction, possibly due to a strong local shear strain applied by the rollers. In addition, nonuniformity

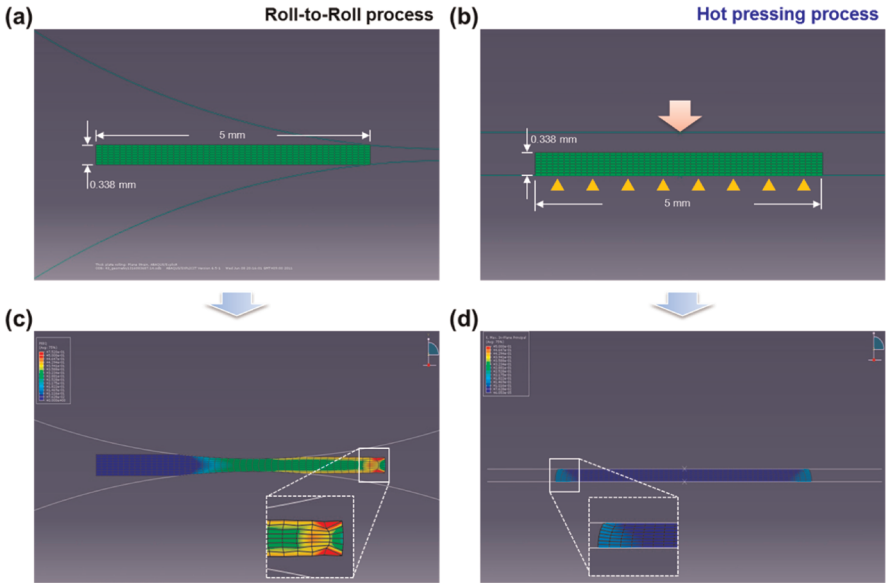

Figure 2. Finite element models of TRT/graphene/PET for (a) R2R and (b) hot pressing processes. The TRT/graphene/PET was modeled as a combined layer with surface friction. The triangles in panel b indicate the directional constraints of fixed mechanical boundaries. (c, d) The resulting strain distributions for R2R and hot pressing processes, respectively.

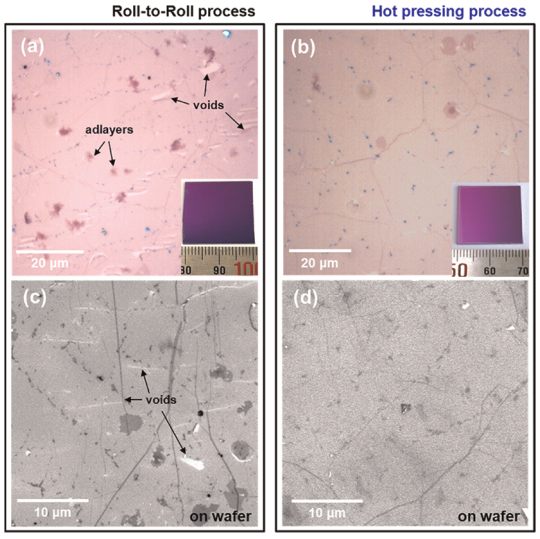

Figure 3. (a, b) Optical and (c, d) scanning electron microscope images showing the surface morphologies of the graphene films transferred onto SiO_2/Si substrates by R2R and hot pressing, respectively.

in heat and pressure causes the inhomogeneous detachment from TRT, resulting in large cracks and voids.[32] On the other hand, the hot pressing method provides the homogeneous distribution of temperature and pressure at large scale.[33,34] Therefore, the density of defects can be minimized by using the hot pressing method, leading to the better electrical properties of graphene. Thus, we can conclude that the electrical properties of graphene depend not only on synthesis and doping processes but on a transfer process minimizing mechanical damages.[9,35−38]

The electrical property of transferred graphene is tested by the four-probe measurement of sheet resistance, and its statistical distribution is shown in Figure 4. The best electrical properties were achieved at ∼125 °C in both transfer methods. The sheet resistance of graphene transferred to a flexible PET by hot pressing shows the narrow distribution around 460 Ohm/square, which is comparable to the R2R transferred sample. However, the sheet resistances of R2R transferred graphene on a rigid substrate (SiO_2/Si) show much larger values than the hot-pressed case, indicating that the R2R method is good for only flexible substrates. This is possibly because the rigid surface cannot absorb the excessive pressure applied to graphene during the R2R process. On the other hand, the hot pressing method works well both for flexible and rigid substrates because of the uniformly distributed mechanical loads on the graphene films. We also tested the electrical properties of randomly stacked 3-layer graphene on PET. The averaged sheet resistance values of graphene transferred by hot pressing ranges from 150 to 162 Ohm/square, while the R2R samples show 210−250 Ohm/square. The electrical enhancement of 3-layer graphene films by hot pressing is not as large as the case of monolayer, because more than two graphene layers are patching their voids and defects each other.

Figure 4b presents the sheet resistance distribution of the graphene film transferred onto a 6 × 6 cm^2 SiO_2/Si wafer. The Gaussian fit yields the averaged sheet resistance of 397.7 Ohm/square and the standard deviation of 53.5 Ohm/square. We also prepare larger graphene films on glass and PET substrates (17−18 in. in diagonal) using hot pressing in order to demonstrate the scalability of the hot pressing method (see Supporting Information, Figure S1). The large-area graphene film on a glass substrate exhibited an averaged sheet

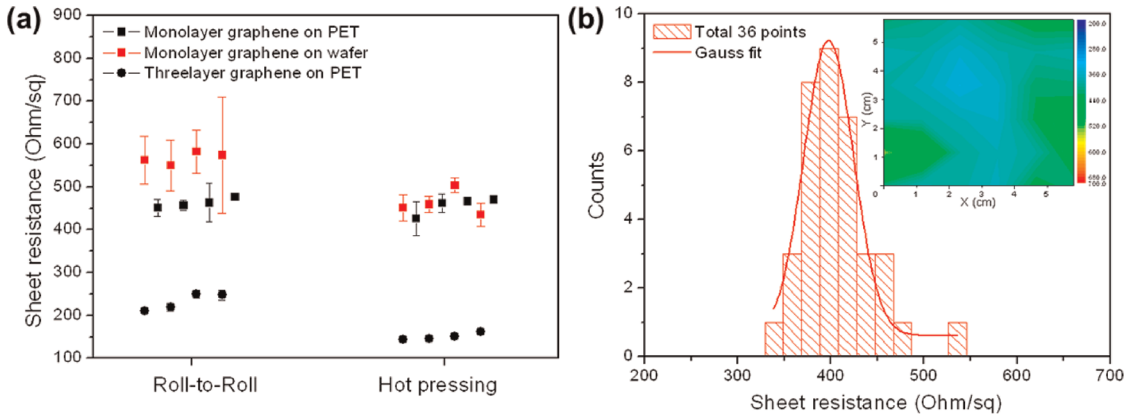

Figure 4. Sheet resistance distribution of graphene films transferred by R2R and hot pressing processes. (a) Sheet resistance distribution of monolayer and three-layer graphene films transferred by R2R and hot pressing. The sheet resistances were measured at four different positions for each graphene sample transferred on 188 μm-thick PET substrates (black squares, black circles) and 500 μm thick SiO_2/Si wafers (red squares). The three-layer graphene films were preapared by a layer-by-layer process at 125 °C, which is an optimal transfer temperature condition both for R2R and hot pressing processes. (b) Sheet resistance histogram of the 6 × 6 cm^2 graphene film on a SiO_2/Si wafer transferred by hot pressing. The inset image shows the corresponding spatial distribution of sheet resistances.

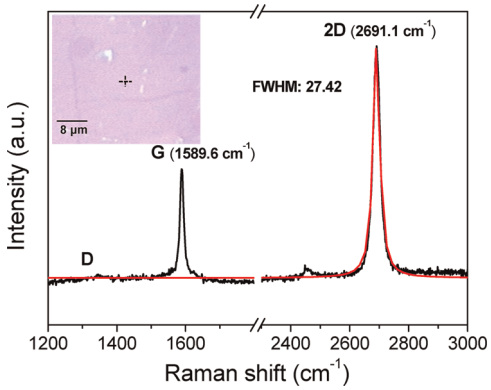

Figure 5. Representative Raman spectrum (excitation wavelength: 514 nm) of the graphene film on a SiO_2/Si substrate transferred by hot pressing. The inset shows the corresponding optical microscope image.

resistance of 373.6 ± 157.2 Ohm/square, which is slightly lower than the graphene film on a PET substrate.

The qualities of the graphene films transferred by hot pressing on a SiO_2/Si wafer were estimated by Raman spectroscopy (Ranishaw, excitation wavelength λ = 514 nm). Figure 5 represents typical characteristics of monolayer graphene: The 2D band centered at ~2691.1 cm^{-1} is symmetric and well-fitted by a single Lorentzian peak shown in red. The full width half-maximum (fwhm) of a 2D peak is 27.42, and the intensity ratio of the 2D band to G band (I_{2D}/I_G) is ~2. Both the I_{2D}/I_G and the fwhm of the 2D band are consistent with those of monolayer graphene.[39] The low density of the D peaks suggests that the graphene film be well-transferred on the wafer without significant damages. We suppose that the occurrence of D peaks is due to the residue of thermal release adhesives or wrinkles formed during the transfer process.[10,23,40]

Although a R2R transfer method using TRT can fabricate a large-scale conductive film, cracks and tears are often found on the graphene film after transfer. This is probably due to strong mechanical strain that is locally applied to the graphene film between the hot rollers. Thus, careful mechanical analyses and simulations on thin conductive films associated with the thickness and flexibility of the substrates are required for the better performance of flexible electronic devices.[11,25,41,42] To validate previous FEM simulation and experiment in smaller scale, we also conducted a coarse-grained simulation using the elastic network model (ENM).[43−45] ENM is one of the most fascinate modeling tools to simulate macromolecular dynamics, in which an atomic structure is represented as a network of virtual springs connecting spatially proximal representative atoms. In Supporting Information, Figure S2, we constructed two graphene models of which the size is 1.6 × 1.6 μm^2 and tested their mechanical behaviors. A hot-pressed sample was modeled as a perfect lattice structure, but the R2R model had a hole of which the shape was mimicked from the AFM image in Figure S2a. The distance between adjacent representative (*i.e.*, sampled) atoms was set to be 40 nm, and two types of virtual spring constants were used to distinguish the primary bond interaction within 40 nm from the secondary bond interaction between 40 and 60 nm. Figure S2e shows the strain distribution plots when the same *y*-directional tensile load is applied to both of the graphene models. In contrast with the Young's modulus calculated from the perfect graphene model which matches the reference value of 1.0 TPa,[7] the other graphene model with a hole has a considerably low Young's modulus of 0.14 TPa. Likewise, Supporting Information, Figure S3 demonstrates the simulation results for atomic scale graphene models with and without defects. The graphene sheets consist of honeycomb units, and each carbon atom is constrained by two types of spring constants: one for

the primary covalent bond between adjacent carbons (within 0.15 nm) and the other for representing non-bonded interactions (between 0.15 and 0.3 nm) under the *y*-directional tensile intensity of 3.417 nN/nm. Supporting Information, Figure S3e apparently shows that the normal strain of the perfect graphene model is smaller than that of the other graphene model with a hole. This theoretical study reveals that the defect control during the dry transfer process is the most important factor to maintain the intrinsic mechanical properties of graphene regardless of its scale.

CONCLUSION

We demonstrated that the hot pressing method improves the transfer efficiency of graphene films on a rigid substrate with arbitrary thickness and rigidity, which are evidenced by otpical, SEM images, Raman spectroscopy, and electrical analyses. The theoretical simulation also reveals that the mechanical strain applied to the graphene on substrates can be minimized and neutralized by using the hot pressing method, while the R2R dry-transfer onto to a rigid substrate results in a large mechanical deformation leading to the formation of cracks and voids. The hot pressing method would be particularly useful for the fabrication of large-area display and touch panel devices on glass substrates that are widely being used for commercial electronics. Therefore, we expect that the practical applications of the graphene-based conductive films replacing indium tin oxides (ITO) will be realized in near future.

EXPERIMENTAL METHODS

Synthesis of Graphene. The graphene was first grown on Cu substrate using 2 in. and 8 in. CVD systems. A Cu foil was inserted into a 2 in. quartz tube with a 2 sccm H_2 flow and then annealed for 1 h 30 min at the high temperature, 1000 °C. Subsequently, a 20 sccm CH_4 flow was inserted for graphene growth and the total pressure was maintained at 30 mTorr for 30 min. After that, the furnace was quickly cooled down to room temperature under He conditions. For the large-area graphene growth, a Cu foil was hung on the U shape holder in an 8 in. CVD system with a mixture of 10 sccm H_2 and 15 sccm CH_4. The back side of graphene on the Cu foil was exposed to the O_2 plasma for exfoliation.

Dry Transfer. The TRT (Nitto Denko) was placed on the graphene film, and then the Cu substrate was etched by ammonia persulfate 0.1 M in etchant box. The Si wafer with 300 nm thermal oxide was exposed to the O_2 plasma for dry cleaning and strong adhesion of silicon substrate to the graphene film. The graphene on TRT was inserted between rollers that enable attachment to target substrates such as PET or SiO_2/Si substrates. The TRT/graphene film/target substrate was inserted into rollers or plates and then was heated up at 125 °C. In the hot pressing process, the normal stress of 4 N/mm^2 is applied to the tape/graphene/substrate for less than 10 s. After the transfer process, the TRT lost adhesion force and then peeled off slowly resulting in the graphene film transferred onto the target substrate.

Characterization. The surface morphology of transferred graphene on SiO_2/Si wafer was investigated by optical microscope (Nikon Eclipse LV100) and field-emission SEM (JEOL, JSM-6390). Raman spectroscopy (Renishaw, 514 nm, Ar^+ ion laser) was used to characterize graphene transferred by the hot pressing method. The sheet resistance of the graphene was measured using a four-point probe with a nanovoltmeter (Keithley 6221, 2182A). Contact-mode AFM images were acquired at the 0.5 Hz scan rate (Park system, XE-100).

Conflict of Interest: The authors declare no competing financial interest.

Supporting Information Available: Additional information on large-area graphene films transferred onto a glass and a PET substrate, coarse-grained and atomic scale simulation of graphene films. This material is available free of charge *via* the Internet at http://pubs.acs.org.

Acknowledgment. The authors are grateful for the support from the World Class University Program (R33-10079), Global Research Lab (GRL) Program (2011-0021972), Center for Advanced Soft Electronics under the Global Frontier Research Program (2011-0031627), and Basic Science Research Program (2011K000615, 2011-0017587, 2009-0083540, 2009-0090017) through the National Research Foundation of Korea funded by the Ministry of Education, Science and Technology. The work presented in this paper was supported in part by Samsung Display Co., Ltd.

REFERENCES AND NOTES

1. Novoselov, K. S.; Geim, A. K.; Morozov, S. V.; Jiang, D.; Zhang, Y.; Dubonos, S. V.; Grigorieva, I. V.; Firsov, A. A. Electric Field Effect in Atomically Thin Carbon Films. *Science* **2004**, *306*, 666–669.
2. Novoselov, K. S.; Geim, A. K.; Morozov, S. V.; Jiang, D.; Katsnelson, M. I.; Grigorieva, I. V.; Dubonos, S. V.; Firsov, A. A. Two-Dimensional Gas of Massless Dirac Fermions in Graphene. *Nature* **2005**, *438*, 197–200.
3. Zhang, Y. B.; Tan, Y. W.; Stormer, H. L.; Kim, P. Experimental Observation of the Quantum Hall Effect and Berry's Phase in Graphene. *Nature* **2005**, *438*, 201–204.
4. Geim, A. K.; Novoselov, K. S. The Rise of Graphene. *Nat. Mater.* **2007**, *6*, 183–191.
5. Li, X.; Zhang, G. Y.; Bai, X. D.; Sun, X. M.; Wang, X. R.; Wang, E.; Dai, H. J. Highly Conducting Graphene Sheets and Langmuir–Blodgett Films. *Nat. Nanotechnol.* **2008**, *3*, 538–542.
6. Avouris, P.; Chen, Z.; Perebeinos, V. Carbon-Based Electronics. *Nat. Nanotechnol.* **2007**, *2*, 605–613.
7. Lee, C.; Wei, X.; Kysar, J. W.; Hone, J. Measurement of the Elastic Properties and Intrinsic Strength of Monolayer Graphene. *Science* **2008**, *321*, 385–388.
8. Wang, Y.; Yang, R.; Shi, Z.; Zhang, L.; Shi, D.; Wang, E.; Zhang, G. Super-Elastic Graphene Ripples for Flexible Strain Sensors. *ACS Nano* **2011**, *5*, 3645–3650.
9. Kim, K. S.; Zhao, Y.; Jang, H.; Lee, S. Y.; Kim, J. M.; Kim, K. S.; Ahn, J.-H.; Kim, P.; Choi, J.-Y.; Hong, B. H. Large-Scale Pattern Growth of Graphene Films for Stretchable Transparent Electrodes. *Nature* **2009**, *457*, 706–710.
10. Bae, S.; Kim, H.; Lee, Y.; Xu, X.; Park, J.; Zheng, Y.; Balakrishnan, J.; Lei, T.; Kim, H.; Song, Y. I.; *et al.* Roll-to-Roll Production of 30-Inch Graphene Films for Transparent Electrodes. *Nat. Nanotechnol.* **2010**, *5*, 574–578.
11. Lee, Y.; Bae, S.; Jang, H.; Jang, S.; Zhu, S.; Sim, S.; Song, Y. I.; Hong, B. H.; Ahn, J.-H. Wafer-Scale Synthesis and Transfer of Graphene Films. *Nano Lett.* **2010**, *10*, 490–493.
12. Blake, P.; Brimicombe, P. D.; Nair, R. R.; Booth, T. J.; Jiang, D.; Schedin, F.; Ponomarenko, L. A.; Morozov, S. V.; Gleeson, H. F.; Hill, E.; *et al.* Graphene-Based Liquid Crystal Device. *Nano Lett.* **2008**, *8*, 1704–1708.
13. Zhang, Y. B.; Small, J. P.; Ponius, W. V.; Kim, P. Fabrication and Electric-Field-Dependent Transport Measurements of Mesoscopic Graphite Devices. *Appl. Phys. Lett.* **2005**, *86*, 073104.
14. Eda, G.; Fanchini, G.; Chhowalla, M. Large-Area Ultrathin Films of Reduced Graphene Oxide as a Transparent and

Flexible Electronic Material. *Nat. Nanotechnol.* **2008**, *3*, 270–274.
15. Stankovich, S.; Dikin, D. A.; Piner, R. D.; Kohlhaas, K. A.; Kleinhammes, A.; Jia, Y.; Wu, Y.; Nguyen, S. T.; Ruoff, R. S. Synthesis of Graphene-Based Nanosheets *via* Chemical Reduction of Exfoliated Graphite Oxide. *Carbon* **2007**, *45*, 1558–1565.
16. Berger, C.; Song, Z.; Li, X.; Wu, X.; Brown, N.; Naud, C.; Mayou, D.; Li, T.; Hass, J.; Marchenkov, A. N.; *et al.* Electronic Confinement and Coherence in Patterned Epitaxial Graphene. *Science* **2006**, *312*, 1191–1196.
17. Hernandez, Y.; Nicolosi, V.; Lotya, M.; Blighe, F. M.; Sun, Z.; De, S.; McGovern, I. T.; Holland, B.; Byrne, M.; Gun'Ko, Y. K.; *et al.* High-Yield Production of Graphene by Liquid Phase Exfoliation of Graphite. *Nat. Nanotechnol.* **2008**, *3*, 563–568.
18. Reina, A.; Jia, X.; Ho, J.; Nezich, D.; Son, H. B.; Bulovic, V.; Dresselhaus, M. S.; Kong, J. Large Area, Few-Layer Graphene Films on Arbitrary Substrates by Chemical Vapor Deposition. *Nano Lett.* **2009**, *9*, 30–35.
19. Li, X. S.; Cai, W. W.; An, J.; Kim, S.; Nah, J.; Yang, D. X.; Piner, R.; Velamakanni, A.; Jung, I.; Tutuc, E.; *et al.* Large-Area Synthesis of High-Quality and Uniform Graphene Films on Copper Foils. *Science* **2009**, *324*, 1312–1314.
20. Bunch, J. S.; Verbridge, S. S.; Alden, J. S.; van der Zande, A. M.; Parpia, J. M.; Craighead, H. G.; McEuen, P. L. Impermeable Atomic Membranes from Graphene Sheets. *Nano Lett.* **2008**, *8*, 2458–2462.
21. Wu, J.; Agrawal, M.; Becerril, H. A.; Bao, Z.; Liu, Z.; Chen, Y.; Peumans, P. Organic Light-Emitting Diodes on Solution-Processed Graphene Transparent Electrodes. *ACS Nano* **2010**, *4*, 43–48.
22. Kang, J.; Kim, H.; Kim, K. S.; Lee, S.; Bae, S.; Ahn, J.-H.; Kim, Y.-J.; Choi, J.-B.; Hong, B. H. High-Performance Graphene-Based Transparent Flexible Heaters. *Nano Lett.* **2011**, *11*, 5154–5158.
23. Li, X. S.; Zhu, Y. W.; Cai, W. W.; Borysiak, M.; Han, B. Y.; Chen, D.; Piner, R. D.; Colombo, L.; Ruoff, R. S. Transfer of Large-Area Graphene Films for High-Performance Transparent Conductive Electrodes. *Nano Lett.* **2009**, *9*, 4359–4363.
24. Caldwell, J. D.; Anderson, T. J.; Culbertson, J. C.; Jernigan, G. G.; Hobart, K. D.; Kub, F. J.; Tadjer, M. J.; Tedesco, J. L.; Hite, J. K.; Mastro, M. A.; *et al.* Technique for the Dry Transfer of Epitaxial Graphene onto Arbitrary Substrates. *ACS Nano* **2010**, *4*, 1108–1114.
25. Unarunotai, S.; Koepke, J. C.; Tsai, C.-L.; Du, F.; Chialvo, C. E.; Murata, Y.; Haasch, R.; Petrov, I.; Mason, N.; Shim, M.; *et al.* Layer-by-Layer Transfer of Multiple, Large Area Sheets of Graphene Grown in Multilayer Stacks on a Single SiC Wafer. *ACS Nano* **2010**, *4*, 5591–5598.
26. Liang, X.; Sperling, B. A.; Calizo, I.; Cheng, G.; Hacker, C. A.; Zhang, Q.; Obeng, Y.; Yan, K.; Peng, H.; Li, Q.; *et al.* Toward Clean and Crackless Transfer of Graphene. *ACS Nano* **2011**, *5*, 9144–9153.
27. Wang, Y.; Zheng, Y.; Xu, X.; Dubuisson, E.; Bao, Q.; Lu, J.; Loh, K. P. Electrochemical Delamination of CVD-Grown Graphene Film: Toward the Recyclable Use of Copper Catalyst. *ACS Nano* **2011**, *5*, 9927–9933.
28. Suk, J. W.; Kitt, A.; Magnuson, C. W.; Hao, Y.; Ahmed, S.; An, J.; Swan, A. K.; Goldberg, B. B.; Ruoff, R. S. Transfer of CVD-Grown Monolayer Graphene onto Arbitrary Substrates. *ACS Nano* **2011**, *5*, 6916–6924.
29. Verma, V. P.; Das, S.; Lahiri, I.; Choi, W. Large-Area Graphene on Polymer Film for Flexible and Transparent Anode in Field Emission Device. *Appl. Phys. Lett.* **2010**, *96*, 203108.
30. Bajpai, R.; Roy, S.; Jain, L.; Kulshrestha, N.; Hazra, K. S.; Misra, D. S. Facile One-Step Transfer Process of Graphene. *Nanotechnology* **2011**, *22*, 225606.
31. Denardin, E. L. G.; Tokumoto, S.; Samios, D. Stress-Strain Behaviour of Poly(ethylene terephthalate) (PET) during Large Plastic Deformation by Plane Strain Compression: The Relation between Stress−Strain Curve and Thermal History, Temperature and Strain Rate. *Rheol. Acta* **2005**, *45*, 142–150.
32. Hagan, E. F.; Dietz, K. H. *Dry Film Lamination Process Effects of Lamination Parameters on Wrinkling and Dimensional Properties of Dry Film and Copper Clad Laminate*. *Proceedings of the IPC Printed Circuit Expo '99*, March 14−18, **1999**; Technical Paper Film S05-2.
33. Hine, P. J.; Ward, I. M.; Teckoe, J. The Hot Compaction of Woven Polypropylene Tapes. *J. Mater. Sci.* **1998**, *33*, 2725–2733.
34. Ward, I. M.; Hine, P. J. The Science and Technology of Hot Compaction. *Polymer* **2004**, *45*, 1413–1427.
35. Yu, Q.; Jauregui, L. A.; Wu, W.; Colby, R.; Tian, J.; Su, Z.; Cao, H.; Liu, Z.; Pandey, D.; Wei, D.; *et al.* Control and Characterization of Individual Grains and Grain Boundaries in Graphene Grown by Chemical Vapour Deposition. *Nat. Mater.* **2011**, *10*, 443–449.
36. Günes-, F.; Shin, H.-J.; Biswas, C.; Han, G. H.; Kim, E. S.; Chae, S. J.; Choi, J.-Y.; Lee, Y. H. Layer-by-Layer Doping of Few Layer Graphene Film. *ACS Nano* **2010**, *4*, 4595–4600.
37. Kasry, A.; Kuroda, M. A.; Martyna, G. J.; Tulevski, G. S.; Bol, A. A. Chemical Doping of Large-Area Stacked Graphene Films for Use as Transparent, Conducting Electrodes. *ACS Nano* **2010**, *7*, 3839–3844.
38. Bhaviripudi, S.; Jia, X.; Dresselhaus, M.; Kong, J. Role of Kinetic Factors in Chemical Vapor Deposition Synthesis of Uniform Large Area Graphene Using Copper Catalyst. *Nano Lett.* **2010**, *10*, 4128–4133.
39. Ferrari, A. C.; Meyer, J. C.; Scardaci, V.; Casiraghi, C.; Lazzeri, M.; Mauri, F.; Piscanec, S.; Jiang, D.; Novoselov, K. S.; Roth, S.; *et al.* Raman Spectrum of Graphene and Graphene Layers. *Phy. Rev. Lett.* **2006**, *97*, 187401.
40. Obraztsov, A. N.; Obraztsova, E. A.; Tyurnina, A. V.; Zolotukhin, A. A. Chemical Vapor Deposition of Thin Graphite Films of Nanometer Thickness. *Carbon* **2007**, *45*, 2017–2021.
41. Ishikawa, F. N.; Chang, H. K.; Ryu, K.; Chen, P.; Badmaev, A.; Gomez, De Arco L.; Shen, G.; Zhou, C. Transparent Electronics Based on Transfer Printed Aligned Carbon Nanotubes on Rigid and Flexible Substrates. *ACS Nano* **2009**, *3*, 73–79.
42. Patil, N.; Lin, A.; Myers, E. R.; Ryu, K.; Badmaev, A.; Zhou, C.; Wong, H. −S. P.; Mitra, S. Wafer-Scale Growth and Transfer of Aligned Single-Walled Carbon Nanotubes. *IEEE Trans. Nanotechnol.* **2009**, *8*, 498–504.
43. Kim, M. K.; Chirikjian, G. S.; Jernigan, R. L. Elastic Models of Conformational Transitions in Macromolecules. *J. Mol. Graph. Model.* **2002**, *21*, 151–160.
44. Kim, M. K.; Jernigan, R. L; Chirikjian, G. S. Efficient Generation of Feasible Pathways for Protein Conformational Transitions. *Biophys. J.* **2002**, *83*, 1620–1630.
45. Kim, M. K.; Jang, Y.; Jeong, J. I. Using Harmonic Analysis and Optimization to Study Macromolecular Dynamics. *Int. J. Control. Autom.* **2006**, *4*, 382–393.